Published in final edited form as:
J Magn Reson Imaging. 2014 April ; 39(4): 958–965. doi:10.1002/jmri.24257.

A Method to Create Regional Mechanical Dyssynchrony Maps from Short-Axis Cine SSFP Images

Jonathan D. Suever, BS[1], **Brandon K. Fornwalt, MD, PhD**[2], **Lee R. Neuman, BS**[1], **Jana G. Delfino, PhD**[3], **Michael S. Lloyd, MD**[4], and **John N. Oshinski, PhD**[1,3]

[1]Wallace H. Coulter Department of Biomedical Engineering, Georgia Institute of Technology/ Emory University, Atlanta, GA

[2]Departments of Pediatrics, Biomedical Engineering and Physiology, University of Kentucky, Lexington, KY

[3]Department of Radiology & Imaging Sciences, Emory University School of Medicine, Atlanta, GA

[4]Division of Cardiology, Department of Medicine, Emory University School of Medicine, Atlanta, GA

Abstract

Purpose—To develop a robust method to assess regional mechanical dyssynchrony from cine short-axis MR images. Cardiac resynchronization therapy (CRT) is an effective treatment for patients with heart failure and evidence of left-ventricular (LV) dyssynchrony. Patient response to CRT is greatest when the LV pacing lead is placed in the most dyssynchronous segment. Existing techniques for assessing regional dyssynchrony require difficult acquisition and/or postprocessing. Our goal was to develop a widely applicable and robust method to assess regional mechanical dyssynchrony.

Materials and Methods—Using the endocardial boundary, radial displacement curves (RDCs) were generated throughout the LV. Cross-correlation was used to determine the delay time between each RDC and a patient-specific reference. Delay times were projected onto the AHA 17-segment model creating a regional dyssynchrony map. Our method was tested in 10 normal individuals and 10 patients enrolled for CRT (QRS>120ms, NYHA III-IV, EF<35%).

Results—Delay times over the LV were 23.9±33.8ms and 93.1±99.9ms ($p<0.001$) in normal subjects and patients, respectively. Inter-observer reproducibility for segment averages was 6.8±39.3ms and there was 70% agreement in identifying the latest contracting segment.

Conclusion—We have developed a method that can reliably calculate regional delay times from cine SSFP images. Maps of regional dyssynchrony could be used to identify the latest-contracting segment to assist in CRT lead implantation.

Keywords

Cardiac Resynchronization Therapy; Mechanical Dyssynchrony; Magnetic Resonance Imaging

Introduction

Intra-ventricular mechanical dyssynchrony results from a dis-coordinate timing of contraction between segments of the left ventricle (LV). This LV dyssynchrony is present in

Corresponding Author: Jonathan D. Suever, BS, Department of Biomedical Engineering, Emory University and Georgia Institute of Technology, 1364 Clifton Road, Suite AG30, Atlanta, Georgia 30322, Tel 256.513.9513, Fax 404.712.5948, suever@gatech.edu.

approximately 30% of patients with heart failure, particularly those with dilated cardiomyopathy and left bundle branch block (LBBB)(1,2). Cardiac resynchronization therapy (CRT) is an effective treatment for patients with heart failure and evidence of electrical dyssynchrony on a surface electrocardiogram. In CRT using bi-ventricular pacing, one lead is placed through the RV into the septal wall and a second lead is placed through the coronary sinus into the lateral wall of the LV. Simultaneous pacing of the leads stimulates coordinated contraction of the septal and lateral regions of the LV to restore synchrony. Although CRT increases survival and improves quality of life in specific heart failure populations(3), ~30% of appropriately selected candidates for CRT do not have measureable improvement in symptoms 6 months after CRT implantation (so-called 'non-responders')(4,5).

The role of *mechanical* dyssynchrony as a predictive tool for CRT response is not well understood. Mechanical dyssynchrony is not currently considered during patient selection despite some evidence showing its ability to select patients who will have a positive response to CRT(6). Echocardiographic techniques such as tissue Doppler imaging (TDI) have been utilized to assess LV mechanical dyssynchrony(7,8). These methods are operator-dependent, require an acoustic window, and exhibit poor reproducibility(9). In large international multi-center trials, echocardiographic measures of dyssynchrony failed to significantly improve CRT patient selection over standard echocardiographic parameters(10).

Placement of the LV lead in the region of latest contraction may have a role in response to CRT. Retrospective studies have shown that patient response to CRT is greatest when the LV pacing lead is placed in the most dyssynchronous or latest-contracting segment(11,12). To discern the relationship between regional mechanical dyssynchrony, lead position, and CRT response, a method to determine regional mechanical dyssynchrony over the LV that can be applied in large multi-center studies must first be developed. A regional map of dyssynchrony could also be used as a tool to plan lead placement.

Several MRI-based methods have been developed in order to provide an assessment of mechanical dyssynchrony. Myocardial tagging can be used for assessing dyssynchrony(13). However, tagging requires specialized acquisition sequences and significant post-processing(14,15) to determine regional dyssynchrony. A number of groups have utilized advanced phase-based techniques such as displacement encoding using stimulated echoes (DENSE)(16–18), tissue velocity mapping (TVM)(19), and strain-encoding (SENC)(20). These techniques can obtain regional dyssynchrony information based on either strain or displacements; however, only specialized centers are capable of performing and analyzing these scans, limiting the feasibility of using these techniques in multi-center dyssynchrony studies.

In contrast to tagging, DENSE, TVM, and SENC, SSFP cine images are part of nearly all standard cardiac MR examinations performed, and SSFP is optimized for both high temporal and spatial resolution acquisitions. SSFP-based methods have been developed to derive regional and global LV motion information from cine images. Previous techniques developed to quantify dyssynchrony are either global measures(21,22), assume that the contraction follows an idealized motion pattern(21), use time-to-peak based measurements reliant on user identification of the end systolic time point (23), or involve complicated post-processing or large training sets (24). Thus these existing techniques are difficult to use for accurate and reproducible regional dyssynchrony analysis.

The goal of this study was to develop a method that utilized SSFP cine images to create regional maps of mechanical dyssynchrony. The method obtains radial displacement curves

(RDCs) from short axis cine images, determines the mechanical activation delay at any location within the left ventricle relative to a patient-specific reference using cross-correlation, and displays this information on a standard AHA 17-segment bullseye model for visualization. By utilizing a patient-specific reference, it is possible to determine which regions contract early and late in each patient. The resultant maps show regional distribution of LV motion and could be used as a guide for lead placement. We applied the method in a study group of subjects with clinical evidence of LV dyssynchrony and compared the measurements to a group of normal controls.

Methods

Study Subjects

This study included 10 control subjects with no history of cardiovascular disease, a normal EKG, and no evidence of electrical dyssynchrony (QRS duration < 120 ms on a 12-Lead EKG), and 10 patients who met accepted clinical criteria for CRT: New York Heart Association (NYHA) Class III or IV heart failure, LV Ejection Fraction (EF) < 35%, QRS Duration > 120 ms, and optimal medical therapy for at least one month. All patients used in this study had a QRS duration > 150 ms (evidence of electrical dyssynchrony) and were responders to CRT as determined by a 15% decrease in LV end systolic volume at 3 months post-implantation. This study was approved by the University's Institutional Review Board.

Image Acquisition

Steady-state free-precession (SSFP) short-axis images were acquired during 8–12 second end-expiration breath holds using a 1.5T Philips Intera scanner and a five-element phase array cardiac coil (Philips Medical Systems, Best, Netherlands). EKG triggering was used to obtain 20 frames per cardiac cycle (reconstructed temporal resolution: 32.6 – 58.8 ms). Eight-millimeter thick slices were acquired with no slice-gap to ensure coverage of the entire left ventricle. Acquisition parameters were: acquired matrix size = 192 × 256, reconstructed matrix size = 256 × 256, field of view = 370 mm, flip angle = 65°, TR = 4 ms, and TE = 2 ms. Vertical long-axis (two-chamber, VLA) and horizontal long-axis (four-chamber, HLA) SSFP cine images were also acquired using the same acquisition parameters.

Post-processing

All processing was performed in Matlab (The MathWorks, Natick, MA, USA). The endocardial border on all short-axis and long-axis images was delineated using an active appearance model-based technique with manual corrections (25,26) (Figure 1A). Each contour was sampled at 100 equally spaced points radially starting at the anterior insertion of the right ventricle. The distance from any point relative to the centroid of the left ventricle was computed over time to obtain an RDC at each point throughout the LV. Each RDC was up-sampled by a factor of 10 and a Gaussian smoothing filter with a width of 12.5% of the time series was applied to the data to minimize the effects of frame-to-frame discrepancies in the endocardial contour. The mechanical delay time relative to a reference RDC was determined for each of these RDCs. These mechanical delay times were then mapped onto the standard AHA bullseye (Figure 1E).

Determination of LV Centroid—The location of the central axis of the LV is known to change over the cardiac cycle. Thus in order to obtain an accurate assessment of regional wall motion, it is necessary to track the central axis of the LV over the cardiac cycle. If a stationary centroid is used, simple translation of the heart within the chest cavity will result in erroneous radial displacement estimations(27,28). To determine the central axis, endocardial boundaries were traced on the two-chamber and four-chamber long axis images.

The mitral valve plane was identified in each long axis view by manual selection of the mitral valve annulus. The apex was determined as the centroid of the bottom 15% of the LV. A line extending from the midpoint of the valve plane to the apex of the left ventricle served as the central axis in the imaging plane of the two-chamber and four-chamber views (Figure 2A–B). Utilizing 3D position information from the DICOM header, the central axis in each view was converted to a plane normal to the imaging plane. The intersection of the planes in 3D space was used as the central axis of the LV. The intersection of this central axis with each short-axis imaging plane for each phase of the cardiac cycle was used as the centroid for that particular slice and phase (Figure 2C).

Reference RDC Determination—To determine whether a given region contracts early or late, the RDC in this region must be compared to a reference ("normal") RDC. This reference RDC could be obtained by taking the global average of all RDCs for each individual. However, a global average includes data from early, normal, and late-contracting segments. This can lead to distortions of the reference RDC, especially in patients with large dyssynchronous regions. Therefore, we used a *patient-specific* reference that preserves as much detail as possible to ensure proper delay time estimation. Additionally, in order to accurately determine regional delay times using cross-correlation, it is assumed that the two samples being compared have similar shape. By using a patient-specific reference, rather than a reference RDC derived from healthy individuals, we can account for inter-patient variability of radial contraction patterns.

To determine the reference RDC in this study, quality threshold (QT) clustering(29) using root-mean-square error (RMSE) was used to cluster all RDCs into groups with similar contraction patterns (Figure 1B). RMSE was computed as shown in Equation 1 where N is the number of samples in each radial displacement curve, and x and y are the RDCs being compared.

$$RMSE = \sqrt{\frac{\sum_{i=1}^{N}(x_i - y_i)^2}{N}} \quad [1]$$

All clusters were constrained to have a maximum RMSE of 33% between any two RDCs in the group. This cutoff value (33%) was obtained empirically by finding the 95% confidence interval of RMSE values in all normal subjects (theoretically no abnormal RDCs). We then assume the largest cluster in each patient is representative of "synchronous" contraction of the LV. By averaging all RDCs in this largest cluster, we obtain a patient-specific reference RDC that preserves as much detail as possible.

Mechanical Activation Delay—Normalized cross-correlation analysis was used to determine the delay time between RDCs throughout the LV and the patient-specific reference RDC. In the cross-correlation analysis, each RDC was shifted in time relative to the reference RDC. At each time shift, correlation with the reference was computed.(30) Normalized cross-correlation for a particular delay time (τ) was computed using equation 2 where N is the total number of samples in each curve, X is the sample RDC, and R is the patient-specific reference RDC.

$$NCC(\tau) = \frac{1}{N-1}\sum_{t}\frac{(X(t-\tau) - \overline{X}) \cdot (R(t) - \overline{R})}{\sigma_X \sigma_R} \quad [2]$$

The shift yielding the highest correlation value with the reference was the delay time for that particular RDC (Figure 1D). Due to the cyclic nature of the data, periodicity was assumed

for cross-correlation. This process was repeated for all RDCs throughout the LV. It is important to note that because the patient-specific reference is an average of a variety of RDCs, the delay time computed for the RDCs used to compute the reference is often non-zero.

Creation of Regional Maps—In order to create a display of the spatial distribution of mechanical contraction delay times throughout the LV, we used a bullseye plot with a superimposed 17-segment AHA model(31). The apical (17^{th}) segment was omitted in our work due to the lack of clear endocardial boundaries at the most apical short-axis slice. Delay times were computed for 100 locations in each slice throughout the LV and mapped to a polar plot with a delay time of 0 (white) indicating synchronous contraction, a positive delay (red) indicating early contraction, and a negative delay (blue) representing a late-contracting segment (Figure 1E).

Dyssynchrony Parameters

Average delay times and the average absolute value of the delay times were computed throughout the LV for all patients. In order to compare our maps to previous parameters, we calculated the Yu index, a common measure of regional dyssynchrony, by dividing the LV into 12 segments, averaging the delay times within each segment, and computing the standard deviation of these segment averages(32). Additionally, the Tissue Synchronization Index (CMR-TSI), a parameter previously determined by MRI from SSFP images, was determined by taking the standard deviation of the average delay times within 16 AHA segments(21).

Reproducibility—Inter-observer reproducibility was assessed in five of the normal subjects and five of the patients. Two observers provided unique contours for all three views (short axis, two-chamber, and four-chamber) and average delay times were computed for each AHA segment. Bland Altman analysis was used to determine the agreement between the AHA segment averages(33). Because a primary benefit of a regional measure of mechanical dyssynchrony in patients undergoing CRT is the ability to identify the latest contracting segment, the two observers' contours were used to create regional dyssynchrony maps and determine the latest contracting segment in each of the subjects. Agreement between the observers was assessed using Cohen κ-coefficient(34). For the reproducibility analysis, it is necessary to exclude akinetic regions. For this reason, only regions where the radial displacement exceeded 2mm (greater than one pixel) were considered.

Results

Regional activation maps were generated for all ten normal subjects and in all ten patients (Figure 3). The *absolute values* of the delay times were 23.9 ± 33.8 ms and 93.1 ± 99.9 ms ($p < 0.001$) in normal and patients, respectively (Figure 4A). The larger value for the patients indicated that they have a wider range of delays over the LV.

Delay times were extracted using the time shift that yielded the largest correlation coefficient between an RDC and the patient-specific reference RDC. These coefficients were 0.95 ± 0.07 (range: 0.27 – 1.0) for normal subjects and 0.88 ± 0.12 (range: 0.19 – 1.0) for patients enrolled for CRT (Figure 4B). These correlation values indicate acceptable confidence in the estimated delay times.

The Yu index was found to be 28.9 ± 15.6 ms in normal compared to 76.1 ± 23.6 ms in patients undergoing CRT ($p < 0.001$), and the CMR-TSI parameter was 27.1 ± 12.8 ms in normals and 76.7 ± 25.0 ms in patients ($p < 0.001$). All metrics were determined to be significantly different between patients and normal subjects.

Averaging delay times over AHA segments, it was possible to identify the latest-contracting segment in all patients undergoing CRT. The latest-contracting segment varied among the study patients (antero-lateral segment in 5 patients, postero-lateral segment in 3 patients, and septal segment in 2 patients).

In the reproducibility analysis, segment delays for two observers differed by 6.8 ± 39.3 ms (Bias: 6.8; CI: 77.1). The latest contracting segment was determined to be the same in all but three patients (kappa: 0.64). In two of the patients where the disagreement occurred, the segments selected by the two observers were neighboring lateral wall segments.

Discussion

This study describes a new method for assessing and displaying regional mechanical dyssynchrony from standard cine CMR images. The method is suitable for widespread use due to reliance on SSFP images present in all standard CMR exams. The absolute value of the delay times in patients were significantly greater than delay times in normal subjects. Additionally, both patients and normal subjects had high correlation coefficients when determining the regional delay times between each regional RDC and the reference RDC indicating confidence in the similarities of the RDCs when shifted in time.

Comparison with previous methods

The delay times obtained in this study agree with published contraction timings obtained with various modalities and methodologies. The CMR-TSI values derived from our regional dyssynchrony data agreed with previous studies by Chalil et al. (27 ± 13 ms vs. 21 ± 8 ms and 77 ± 25 ms vs. 106 ± 55.8 ms for normal subjects and patients, respectively).(21) The Yu index of 76.1 ± 23.6 ms in this study was slightly lower than those previously presented found using 3D speckle tracking (124 ± 88 ms)(35). This discrepancy could be due to the lower temporal resolution data provided by MRI compared to that of echocardiography. Higher frame-rate cines could be employed to further explore this discrepancy.

In our study cohort, the location of the latest contracting segment of the left ventricle varied widely. Prior studies have reported conflicting results when identifying the region of the LV most commonly associated with late contraction (35–37). Although our dataset is small, it agrees with more recent data from the MADIT-CRT study which showed widely varying regions of latest delay across study populations (38). In our group, two patients were shown to have the latest contracting segment in the septum, which appears paradoxic to what is typically expected in LBBB patients. In these two patients, there was a very early inward motion of the septum, known as septal flash which is often presented in patients with LBBB (39). In a patient with septal flash, the septal segments undergo two separate displacements during systole. The first results in a small, very early displacement of the septum (prior to myocardial thickening) followed by a much larger displacement when the rest of the ventricle contracts. Due to the nature of our method, in these individuals, the early displacement was not seen by the cross-correlation algorithm as early contraction and thus the second, later inward motion of the septal segments were labeled as late contraction. Based on our convention it appears that those with the “septal flash” or “septal bounce” phenomenon truly have late septal, rather than lateral, thickening and contraction.

We cannot compare the reproducibility of our method to existing MR or echocardiographic techniques due to the lack of reproducibility information from other studies. The inter-observer reproducibility between the two observers was 6.8 ± 39.3 ms (Bias: 6.8; CI: 77.1). The bias is very close to zero indicating good agreement. The fairly large confidence interval is due to the variability in the segment delays seen across patients and normal subjects and is on the order of the temporal resolution of the data (~50 ms). Higher temporal

resolution scans should be utilized to further improve the reproducibility of these scans. The exact same AHA segment was identified as the latest contracting segment in all but three of the patients, and in two of those patients, the neighboring lateral segment was selected. Previous studies have shown that LV leads placed in segments adjacent to the most-delayed segment demonstrated improved response(40). The high reproducibility of this method in determining the latest-contracting segment is necessary for utilizing regional dyssynchrony information for LV lead placement planning.

Correction for gross translation

We utilized a floating centroid based upon endocardial contours on two and four-chamber images in order to compensate for translational motion of the LV. The floating centroid is a well-known issue for LV dyssynchrony assessment(41–43). Without compensation, translation of the heart will result in apparent relaxation of one side of the ventricle (translation away from the centroid), while the other side of the ventricle will appear to exhibit strong contraction (translate toward the centroid). This will produce irregular RDCs, which could result in false delay detection. Various methods have been used in computed tomography(44) and echocardiography(27) to deal with the floating centroid; however, no one has utilized long axis cine information as presented in this study. Due to the fact that the short-axis and long-axis images are acquired at different times, patient movement and respiration can potentially cause misalignment between these images. In this study, no such error was present, but if necessary, the endocardial contour of the two-chamber image and short-axis images could be registered to account for respiratory motion.

Patient-specific reference RDC

Chalil, et al. have previously used the earliest contracting RDC as a reference(21). Using the earliest contracting RDC has several potential drawbacks including the reliance on a single RDC, and the use of a potentially irregular reference. Using a single RDC can result in poor reproducibility due to the fact that two observers could produce very different reference RDCs, which are then used directly to compute all delays (45). Another danger of using the earliest contracting RDC is that it could possibly be an irregular curve as is often the case in patients undergoing CRT (e.g. in a patient with septal flash). It is difficult to do any meaningful comparison with such an RDC because cross-correlation analysis assumes that the shape of the RDCs is relatively similar. In our method, we combine the detail-preserving power of clustering and the smoothing effect of averaging the largest cluster. Using our method, one can discern early and late contraction from normal contraction, such as is present in patients with septal flash or post-systolic contraction(39,46). Our clustering technique ensures that the reference RDC is representative of the majority of the left ventricle.

Detection of akinetic segments

One of the primary limitations of displacement-based methods utilizing endocardial boundaries on short-axis cines (as opposed to strain-based methods) is the inability to identify akinetic regions. Active myocardium surrounding the affected region may cause the endocardial border segment to move, resulting in an RDC regardless of the viability of the tissue. Using cross-correlation to determine delay times, however, enables us to not only obtain a time delay between two RDCs, but also provides a correlation value that is indicative of similarity. In akinetic segments, the correlation would be computed between the reference RDC and essentially a flat line, but the corresponding correlation would be low compared to correlations of other RDCs. As expected, the correlations were lower in patients due to the complexity of the RDCs as well as the influence of potentially akinetic regions.

Future directions and applications

By displaying the regional dyssynchrony information onto a polar (bullseye) map and on the standard AHA 17-segment model, dyssynchrony information can be superimposed with other regional measures of cardiac function or tissue characteristics such as scar or edema. Therefore, one could correlate akinetic or late-contracting segments with scar transmurality information from late gadolinium enhancement MRI(47).

Higher frame-rate imaging could be employed to obtain finer resolution of mechanical delay times.

Although this study utilized 2D radial displacement information, it could easily be applied to three-dimensional data. The extension of this research to 3D data would allow for the detection of both radial and longitudinal dyssynchrony.

Limitations

Since we use short-axis images for dyssynchrony analysis, we are only making a *radial* dyssynchrony map, and longitudinal, through-plane, and torsional motion is not considered. The lack of longitudinal dyssynchrony detection is not a large limitation due to the fact that other studies have not observed significant changes in longitudinal dyssynchrony after CRT device implantation.(48,49) Additionally, by expanding this method to 3D, it could potentially be used to detect both longitudinal and radial dyssynchrony.

Our utilization of a patient-specific reference RDC assumes that the patient has some synchronous contraction remaining in the left ventricle. We believe that this is a valid assumption since any dyssynchronous RDCs will have a wide variance of contraction patterns, while the normal RDCs, even if small in number, will be more similar to each other, and will thus be clustered effectively.

This study didn't utilize age-matched controls and as a result, age-based differences could be a factor in the differences observed between patients and normal subjects.

In conclusion, we presented a method to create regional mechanical activation maps by analyzing RDCs from cine SSFP images using a moving centroid and cross-correlation analysis. This method shows significant differences in measures of dyssynchrony in those with clinical evidence of dyssynchrony compared to controls. Our data supports this method as a potentially useful preoperative tool to guide LV lead placement for CRT.

Acknowledgments

Grant Support:

The authors would like to thank Susan Eder, RT(MR) for assisting with image acquisition. Funding for this research was provided by AHA Grant-in-Aid (JNO), the National Science Foundation Graduate Research Fellowship Program (JDS), and by the National Center for Advancing Translational Sciences of the National Institutes of Health Award Number UL1TR000454.

References

1. Trautmann SI, Kloss M, Auricchio A. Cardiac resynchronization therapy. Current Cardiology Reports. 2002; 4:371–8. [PubMed: 12169233]
2. Baldasseroni S, Opasich C, Gorini M, et al. Left bundle-branch block is associated with increased 1-year sudden and total mortality rate in 5517 outpatients with congestive heart failure: A report from the Italian network on congestive heart failure. Am Heart J. 2002; 143:398–405. [PubMed: 11868043]

3. Cleland JGF, Daubert J-C, Erdmann E, et al. The effect of cardiac resynchronization on morbidity and mortality in heart failure. N Engl J Med. 2005; 352:1539–49. [PubMed: 15753115]
4. Tang ASL, Ellenbogen Ka. A futuristic perspective on clinical studies of cardiac resynchronization therapy for heart failure patients. Curr Opin Cardiol. 2006; 21:78–82. [PubMed: 16470139]
5. Birnie DH, Tang AS. Theproblem of non-response to cardiac resynchronization therapy. Curr Opin Cardiol. 2006; 21:20–6. [PubMed: 16355025]
6. Bax JJ, Abraham T, Barold SS, et al. Cardiac resynchronization therapy: Part 1--issues before device implantation. J Am Coll Cardiol. 2005; 46:2153–67. [PubMed: 16360042]
7. Soliman OII, Geleijnse ML, Theuns DAMJ, et al. Usefulness of left ventricular systolic dyssynchrony by real-time three-dimensional echocardiography to predict long-term response to cardiac resynchronization therapy. Am J Cardiol. 2009; 103:1586–91. [PubMed: 19463520]
8. Gorcsan J, Tanabe M, Bleeker GB, et al. Combined longitudinal and radial dyssynchrony predicts ventricular response after resynchronization therapy. J Am Coll Cardiol. 2007; 50:1476–83. [PubMed: 17919568]
9. Kapetanakis S, Kearney MT, Siva a, Gall N, Cooklin M, Monaghan MJ. Real-time three-dimensional echocardiography: a novel technique to quantify global left ventricular mechanical dyssynchrony. Circulation. 2005; 112:992–1000. [PubMed: 16087800]
10. Chung ES, Leon AR, Tavazzi L, et al. Results of the Predictors of Response to CRT (PROSPECT) trial. Circulation. 2008; 117:2608–16. [PubMed: 18458170]
11. Butter C, Auricchio A, Stellbrink C, et al. Effect of Resynchronization Therapy Stimulation Site on the Systolic Function of Heart Failure Patients. Circulation. 2001; 104:3026–9. [PubMed: 11748094]
12. Bogaard MD, Doevendans P a, Leenders GE, et al. Can optimization of pacing settings compensate for a non-optimal left ventricular pacing site? Europace. 2010; 12:1262–9. [PubMed: 20562112]
13. Zerhouni EA, Parish DM, Rogers WJ, Yang A, Shapiro EP. Human heart: tagging with MR imaging--a method for noninvasive assessment of myocardial motion. Radiology. 1988; 169:59–63. [PubMed: 3420283]
14. Osman NF, Kerwin WS, McVeigh ER, Prince JL. Cardiac motion tracking using CINE harmonic phase (HARP) magnetic resonance imaging. Magn Reson Med. 1999; 42:1048–60. [PubMed: 10571926]
15. Xu C, Pilla JJ, Isaac G, et al. Deformation analysis of 3D tagged cardiac images using an optical flow method. J Cardiovasc Magn Reson. 2010; 12:19. [PubMed: 20353600]
16. Aletras AH, Ding S, Balaban RS, Wen H. DENSE: displacement encoding with stimulated echoes in cardiac functional MRI. J Magn Reson. 1999; 137:247–52. [PubMed: 10053155]
17. Gilson WD, Yang Z, French Ba, Epstein FH. Measurement of myocardial mechanics in mice before and after infarction using multislice displacement-encoded MRI with 3D motion encoding. Am J Physiol -Heart C. 2005; 288:H1491–7.
18. Epstein FH. MRI of left ventricular function. Journal of Nuclear Cardiology: Official Publication of the Am Soc Nucl Cardiol. 2007; 14:729–44.
19. Delfino JG, Bhasin M, Cole R, et al. Comparison of myocardial velocities obtained with magnetic resonance phase velocity mapping and tissue Doppler imaging in normal subjects and patients with left ventricular dyssynchrony. J Magn Reson Imaging. 2006; 24:304–11. [PubMed: 16786564]
20. Pan L, Stuber M, Kraitchman DL, Fritzges DL, Gilson WD, Osman NF. Real-time imaging of regional myocardial function using fast-SENC. Magn Reson Med. 2006; 55:386–95. [PubMed: 16402379]
21. Chalil S, Stegemann B, Muhyaldeen S, et al. Intraventricular dyssynchrony predicts mortality and morbidity after cardiac resynchronization therapy: a study using cardiovascular magnetic resonance tissue synchronization imaging. J Am Coll Cardiol. 2007; 50:243–52. [PubMed: 17631217]
22. Fornwalt BK, Gonzales PC, Delfino JG, Eisner R, León AR, Oshinski JN. Quantification of left ventricular internal flow from cardiac magnetic resonance images in patients with dyssynchronous heart failure. J Magn Reson Imaging. 2008; 28:375–81. [PubMed: 18666147]

23. Rüssel IK, Zwanenburg JJM, Germans T, et al. Mechanical dyssynchrony or myocardial shortening as MRI predictor of response to biventricular pacing? J Magn Reson Imaging. 2007; 26:1452–60. [PubMed: 17968903]
24. Boyer, K.; Gotardo, P.; Saltz, J.; Raman, SV. On the Detection of Intra-Ventricular Dyssynchrony in the Left Ventricle from Routine Cardiac MRI. 3rd IEEE International Symposium on Biomedical Imaging: Macro to Nano; 2006. p. 169-72.
25. Van der Geest RJ, Lelieveldt BPF, Angelié E, et al. Evaluation of a new method for automated detection of left ventricular boundaries in time series of magnetic resonance images using an Active Appearance Motion Model. J Cardiovasc Magn Reson. 2004; 6:609–17. [PubMed: 15347125]
26. Uzümcü M, Van der Geest RJ, Swingen C, Reiber JHC, Lelieveldt BPF. Time continuous tracking and segmentation of cardiovascular magnetic resonance images using multidimensional dynamic programming. InvestRadiol. 2006; 41:52–62.
27. Pearlman JD, Hogan RD, Wiske PS, Franklin TD, Weyman AE. Echocardiographic definition of the left ventricular centroid. I. Analysis of methods for centroid calculation from a single tomogram. J Am Col Cardiol. 1990; 16:986–92.
28. Azhari H, Sideman S, Weiss JL, et al. Three-dimensional mapping of acute ischemic regions using MRI: wall thickening versus motion analysis. Am J Physiol. 1990; 259:H1492–503. [PubMed: 2240248]
29. Heyer LJ. Exploring Expression Data: Identification and Analysis of Coexpressed Genes. Genome Res. 1999; 9:1106–15. [PubMed: 10568750]
30. Oppenheim, AV.; Schafer, RW.; Buck, JR. Discrete-Time Signal Processing. 2. Prentice Hall; 1999.
31. Cerqueira MD. Standardized Myocardial Segmentation and Nomenclature for Tomographic Imaging of the Heart: A Statement for Healthcare Professionals From the Cardiac Imaging Committee of the Council on Clinical Cardiology of the American Heart Association. Circulation. 2002; 105:539–42. [PubMed: 11815441]
32. Yu C-M. Tissue Doppler Echocardiographic Evidence of Reverse Remodeling and Improved Synchronicity by Simultaneously Delaying Regional Contraction After Biventricular Pacing Therapy in Heart Failure. Circulation. 2002; 105:438–45. [PubMed: 11815425]
33. Bland JM, Altman D. Statistical methods for assessing agreement between two methods of clinical measurement. The Lancet. 1986; 47:931–6.
34. Hulley, SB.; Cummings, SR.; Browner, WS.; Grady, D.; Hearst, N.; Newman, TB. Designing Clinical Research. 2. Philadelphia: Lippincott Williams & Wilkins; 2001.
35. Tanaka H, Hara H, Saba S III, JG. Usefulness of three-dimensional speckle tracking strain to quantify dyssynchrony and the site of latest mechanical activation. Am J Cardiol. 2009; 105:235–42. [PubMed: 20102925]
36. Ansalone G, Giannantoni P, Ricci R, Trambaiolo P, Fedele F, Santini M. Doppler myocardial imaging to evaluate the effectiveness of pacing sites in patients receiving biventricular pacing. J Am Col Cardiol. 2002; 39:489–99.
37. Van Bommel RJ, Ypenburg C, Mollema Sa, et al. Site of latest activation in patients eligible for cardiac resynchronization therapy: Patterns of dyssynchrony among different QRS configurations and impact of heart failure etiology. Am Heart J. 2011; 161:1060–6. [PubMed: 21641351]
38. Singh JP, Klein HU, Huang DT, et al. Left Ventricular Lead Position and Clinical Outcome in the Multicenter Automatic Defibrillator Implantation Trial-Cardiac Resynchronization Therapy (MADIT-CRT) Trial. Circulation. 2011; 123:1159–66. [PubMed: 21382893]
39. Duckett SG, Camara O, Ginks MR, et al. Relationship between endocardial activation sequences defined by high-density mapping to early septal contraction (septal flash) in patients with left bundle branch block undergoing cardiac resynchronization therapy. Europace. 2012; 14:99–106. [PubMed: 21752827]
40. Khan FZ, Virdee MS, Palmer CR, et al. Targeted left ventricular lead placement to guide cardiac resynchronization therapy: the TARGET study: a randomized, controlled trial. J Am Col Cardiol. 2012; 59:1509–18.

41. Duan Q, Angelini E, Homma S, Laine A. Tracking endocardium using optical flow along iso-value curve. Conference Proceedings: Annual International Conference of the IEEE Engineering in Medicine and Biology Society IEEE Engineering in Medicine and Biology Society Conference. 2006; 1:707–10. [PubMed: 17946418]

42. Ortega M, Triedman JK, Geva T, Harrild DM. Relation of left ventricular dyssynchrony measured by cardiac magnetic resonance tissue tracking in repaired tetralogy of fallot to ventricular tachycardia and death. Am J Cardiol. 2011; 107:1535–40. [PubMed: 21414597]

43. Li Y, Garson CD, Xu Y, French Ba, Hossack Ja. High frequency ultrasound imaging detects cardiac dyssynchrony in noninfarcted regions of the murine left ventricle late after reperfused myocardial infarction. Ultrasound MedBiol. 2008; 34:1063–75.

44. Gerber TC, Schmermund a, Reed JE, et al. Use of a new myocardial centroid for measurement of regional myocardial dysfunction by electron beam computed tomography: comparison with technetium-99m sestamibi infarct size quantification. Invest Radiol. 2001; 36:193–203. [PubMed: 11283416]

45. Mischi M, Van Den Bosch HM, Jansen AM, Sieben M, Aarts RM, Korsten HM. Quantification of regional left ventricular dyssynchrony by magnetic resonance imaging. IEEE Trans Biomed Eng. 2008; 55:985–95. [PubMed: 18334390]

46. Skulstad H. Postsystolic Shortening in Ischemic Myocardium: Active Contraction or Passive Recoil? Circulation. 2002; 106:718–24. [PubMed: 12163433]

47. Termeer M, Bescós J, Breeuwer M, Vilanova A, Gerritsen F, Gröller E. 1104 The volumetric bull's eye plot. J Cardiovasc Magn Reson. 2008; 10:A229.

48. Helm RH, Leclercq C, Faris OP, et al. Cardiac dyssynchrony analysis using circumferential versus longitudinal strain: implications for assessing cardiac resynchronization. Circulation. 2005; 111:2760–7. [PubMed: 15911694]

49. Sade LE, Demir O, Atar I, Müderrisoglu H, Ozin B. Effect of mechanical dyssynchrony and cardiac resynchronization therapy on left ventricular rotational mechanics. Am J Cardiol. 2008; 101:1163–9. [PubMed: 18394452]

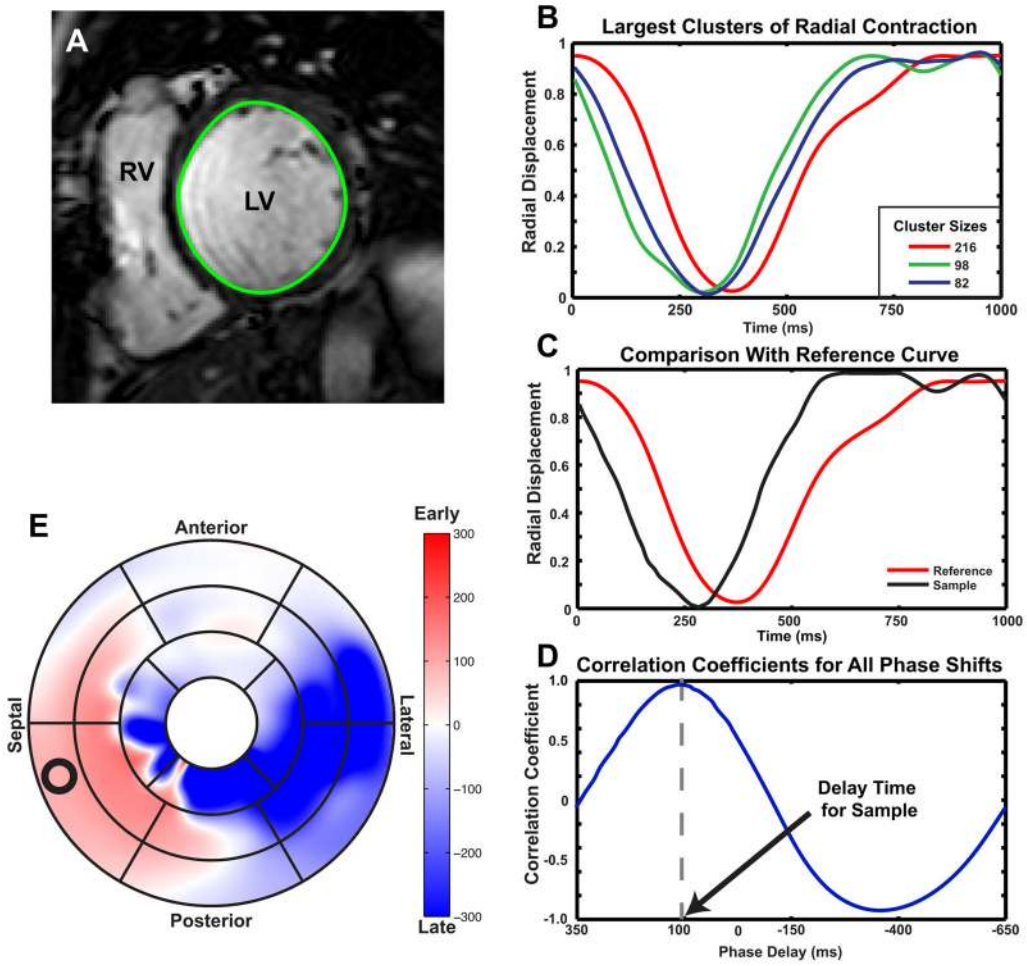

Figure 1. Determination of Mechanical Activation Delays in the Left Ventricle

Using endocardial borders (A), RDCs were computed and clustered using QT clustering (B). The largest cluster was considered to be the patient-specific reference to which all other RDCs were compared (C). The delay time between any RDC and the reference was computed using cross-correlation (D). The delay times throughout the LV were then mapped to the standard AHA bullseye (E).

Figure 2. Determination of Left Ventricular Central Axis from Two and Four-Chamber Images

The location of the mitral valve plane and the central axis of the left ventricle were defined in the four-chamber (A) and two-chamber (B) image planes. Using position information from the DICOM header, this data was projected into three-dimensional space (C) and the intersection of the central axis with the short-axis image plane was defined as the centroid for that particular slice and phase (black arrow).

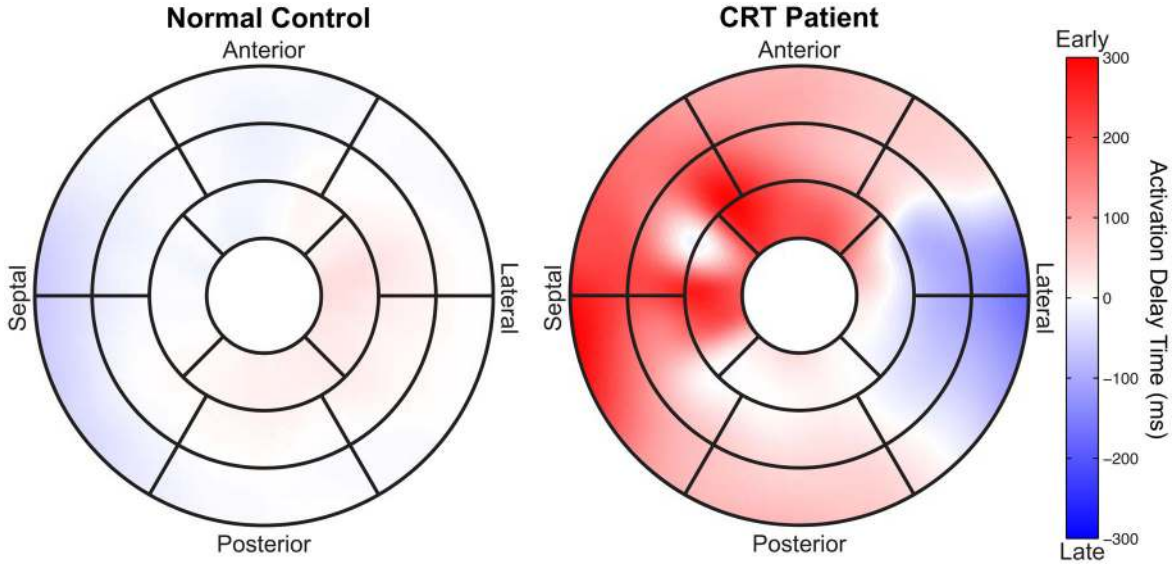

Figure 3. Representative Regional Dyssynchrony Maps

Representative AHA 17-Segment Models of regional delay times for both normal controls (left) and patients undergoing CRT (right)

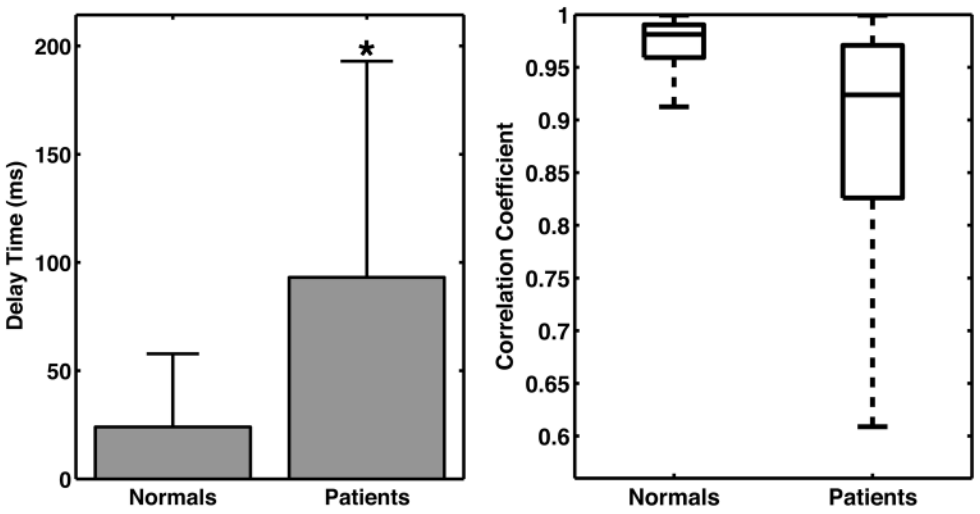

Figure 4. Delay Times and Correlation Values in Healthy Individuals and Patients

Average absolute delay times in normals and patients (left) were significantly different ($p < 0.001$). Normalized cross-correlation coefficients computed between the RDCs and the patient-specific reference RDCs.